Raman scattering from ion-implanted diamond, graphite, and polymers

E. H. Lee
Metals and Ceramics Division, Oak Ridge National Laboratory, Oak Ridge, Tennessee 37830

D. M. Hembree, Jr.
Oak Ridge Y-12 Plant, Martin Marietta Energy System, Inc., Oak Ridge, Tennessee 37831

G. R. Rao and L. K. Mansur
Metals and Ceramics Division, Oak Ridge National Laboratory, Oak Ridge, Tennessee 37830
(Received 4 September 1992; revised manuscript received 10 May 1993)

Raman scattering studies were carried out to investigate the effects of ion implantation on the structure of diamond, graphite, and polymers. Carbon phases produced by chemical vapor deposition (CVD diamond) and rf discharge (diamondlike carbon or DLC) were also analyzed. Two types of amorphous carbon phases were distinguished with relevance to hardness. In general, amorphous carbon phases produced by electron beam evaporation and sputtering are soft (hardness $\ll 1$ GPa), while DLC and some ion-beam-modified polymers are much harder. In all cases, the characteristic Raman bands of the starting material were lost upon ion implantation, and for the lowest fluences the one-phonon bands near 1360 cm^{-1} (D line) and 1580 cm^{-1} (G line) of disordered polycrystalline graphite appeared. With increasing fluence these bands coalesced into a broad, asymmetric peak with the D line shifting to higher wave number and the G line shifting to lower wave number. This trend was clearly distinguishable from the finite crystallite size effect seen in graphite, where, in addition to the appearance of the D line, the G line shifts to higher wave number with decreasing crystallite sizes. Raman scattering could not distinguish between soft and hard amorphous carbon. There was also no indication that the hardness of DLC films and ion-beam-modified polymers was due to diamondlike sp^3 bonds. Instead, hardness in these materials is related to the three-dimensional interconnectivity of chemical bonds. Experimental results suggest that the amorphous carbons examined in this study are composed of random networks of distorted sp, sp^2, and sp^3 bonded atoms, sometimes in a hydrogenated state. The hard carbons such as DLC films and ion beam modified polymers have long-range chemical connectivity while the soft carbons such as damaged graphite, and carbon films prepared by sputter deposition lack such connectivity.

I. INTRODUCTION

In the past decade, hard carbon films such as diamondlike carbon (DLC) and chemical vapor deposited (CVD) diamond have received a great deal of attention in the research community because of potential uses in optical, electronic, and tribological applications.[1-3] Ion implantation of polymers to produce surface films has also been under investigation recently. In our studies,[4-6] it has been discovered that some of the ion-beam-treated polymers become carbon rich and show substantial improvements in tribological properties and hardness (which has increased by factors as great as 50 in some cases). Other researchers have also found carbon enrichment in ion-implanted polymers.[7,8] Many investigators have studied these carbon-based materials in an effort to understand their unusual properties.[9-17]

The nature of the bonding in these materials is key to understanding their properties. Although fourfold coordinated sp^3 diamond bonds have been unambiguously identified in CVD diamond films, the determination of the nature of the bonding (the underlying cause of hardness variations) in DLC, other amorphous carbons and ion-implanted polymers has not been conclusive. In particular, the difference in chemical bonding between the softer and harder amorphous carbon phases has not been resolved, and attempts to correlate hardness to the existence sp^3 diamondlike bonds have not established such a link.

In the present work, ion implantation was carried out on diamond, graphite, and selected polymers. Various ion species, fluences, and energies were employed for implantation. A range of carbonaceous materials, including unhydrogenated amorphous carbon (a-C), DLC, and CVD diamond were also prepared by various methods. Raman scattering studies were performed for the implanted materials as well as for the DLC and CVD films. Hardness data were also collected for most of the samples. The primary motivation for this work was to clarify the nature of the chemical bonding in these carbon-based materials to gain a greater understanding of their material properties.

II. EXPERIMENT

The various carbon-based materials used in this study are listed in Table I. Type-IIa natural diamond with (111) orientation, high grade polycrystalline graphite, commercial grade polyacetal resin (DuPont, Delrin 500®), and polystyrene (PS) were subjected to ion-beam treatments. Implantations were carried out using the multiple ion-beam irradiation facility at Oak Ridge National Laboratory equipped with three Van de Graaff ac-

TABLE I. Summary of ion-implantation conditions.

Materials	Ion species	Energy (keV)	Fluence (ions/m^2)
Diamond	Ar^+	1000	2×10^{20}
Graphite	Si^+	200	1.6×10^{19}
Polyacetal	Ar^+	1000	1.6×10^{20}
Polystyrene	Ar^+	200	8×10^{18}
			2.7×10^{19}
			5.4×10^{19}
		1000	8×10^{18}
			2.7×10^{19}
			5.4×10^{19}
Tefzel	B,N,C	420,700,640	1.2×10^{20} (total fluence)

celerators producing energies up to 5, 2.5, and 0.4 MeV.[18] The beam lines are configured to bombard a target with three ion species simultaneously or independently. During implantation of all samples in this work, beam currents were maintained less than 100 mA/m^2 in order to keep the sample temperature below 50 °C (as confirmed by a thermocouple attached to the sample holder). Also included in this study are the previously reported results[4] for Tefzel®, a copolymer of ethylene and tetrafluoroethylene, which was implanted simultaneously with 420-keV B, 700-keV N, and 604-keV C ion beams to an equal fluence for each species, 1.2×10^{20} ions/m^2. The implantation conditions are summarized in Table I. The amorphous DLC film was prepared on a polystyrene substrate by rf discharge under 25-mTorr CH_4 and Ar with 600-V bias. Polycrystalline diamond films were grown on a silicon substrate by a filament assisted chemical vapor deposition method at 1050 °C under 40-Torr pressure of 1% CH_4 in H_2.

Raman spectra were obtained using an Instruments S A Ramanor U1000 spectrometer. The excitation source was the 514.532-nm line of a Coherent Model Innova 90-5 argon-ion laser typically operated at 100 mW for graphite and 5 mW for the various polymers. The low laser power was necessary for the polymers to avoid thermal damage from excessive absorption of laser radiation. The spectrometer bandpass was typically 9.4 cm^{-1}, and microsampling (180° backscatter geometry) was accomplished with a Leitz 100× objective with a numerical aperture of 0.9. With this objective, the laser beam focal point diameter was approximately 1 μm. Spectra were obtained from 50 to 3500 cm^{-1}. The bandfitting results reported in this work were obtained using an algorithm that optimized both the Gaussian and Lorentzian contributions to the line shape.

III. RESULTS

A. Raman spectroscopy

1. Graphite

Since Raman spectra of ion-beam-modified polymers have their origins in their carbonaceous backbone structure and resemble the spectra of disordered graphite,[4] the Raman spectrum of polycrystalline graphite (100–200-μm grain size) was examined first and is shown in Fig. 1(a). The first-order Raman peak of unimplanted graphite shows a sharp, intense peak at 1580 cm^{-1} (G line), and is assigned to the C-C stretching mode within the graphite basal plane with E_{2g} symmetry.[19,20] The 1354-cm^{-1} disorder peak (D line) results from first-order Raman scattering from a zone edge phonon with A_{1g} symmetry. This normally forbidden Raman mode becomes active as a result of relaxation of the wave-vector conservation selection rule, probably as a result of microcrystallinity.[21] The relationship between the D and G lines has been examined by many researchers and can be related directly to the structure and properties of graphite.[19] A peak near 50 cm^{-1}, which is assigned to a shear type rigid layer mode,[21] was not observed in these experiments.

The second-order spectrum of polycrystalline graphite[20] exhibited four distinct bands, two overtones at $2(1354)\approx2716$ cm^{-1} and $2(1620)\approx3248$ cm^{-1}, and two combination bands at $(1354+1580)\approx2950$ cm^{-1} and $(850+1580)\approx2452$ cm^{-1}. Bands at 850 and 1620 cm^{-1} correspond to peaks in the one-phonon density of states for graphite that are not normally allowed in Raman scattering because of the wave-vector conservation selection rule.[22,23] However, these phonons are allowed in two-phonon Raman scattering. A broad peak near 760 cm^{-1} was not assigned, but probably is due to an instrumental artifact in combination with scattering from nonzone-center phonons.

Upon implantation with 200-keV Si^+ ions to 1.6×10^{19} ions/m^2, all peaks were broadened with a concurrent reduction in the peak heights, making some of the second-order peaks unnoticeable as shown in Fig. 1(b). The peak broadening is caused primarily by phonon damping and, as such, is intimately related to the degree of structural disorder.[11,24] At this fluence, the G line softened slightly to 1578 cm^{-1} while the D line moved higher in frequency from 1354 to 1362 cm^{-1}.

2. Diamond

Figure 2 compares the Raman spectra of diamond before and after implantation with 1000-keV Ar^+. The single triply degenerate first-order Raman peak[25] appeared at 1334 cm^{-1}. For pristine diamond, second-order peaks corresponding to overtones and combination bands[26] were also observed at 2184, 2468, and 2652 cm^{-1}. The second-order peaks were more than 2 orders of magnitude weaker than the first-order band as indicated in Fig. 2. Ion implantation resulted in a complete loss of the Raman bands characteristic of crystalline diamond. Instead, a broad asymmetric peak appeared near 1546 cm^{-1}. Bandfitting revealed that this spectrum was a composite of two peaks, the D line shifted to 1417 cm^{-1} and the G line at 1569 cm^{-1}. The results of the bandfitting analysis are summarized in Table II.

The surface became very dark but was still shiny despite the displacement damage caused by the bombardment. Rutherford backscattering (RBS) and ion channeling analysis exhibited about a 25% increase in back-

scatter yield from the subsurface region[27] which was attributed to lattice atom displacements. The fraction of displaced carbon atoms from sp^3 bonding sites was estimated to be less than $10\pm5\%$.[28] Raman scattering did not show any evidence of the crystalline structure associated with the original diamond lattice.

3. DLC film

The Raman spectrum for the DLC film showed a broad asymmetric peak near 1526 cm^{-1} as shown in Fig. 3. Bandfitting of the asymmetric peak indicated the presence of the *D* line at 1357 cm^{-1} and the *G* line at 1533 cm^{-1} as summarized in Table II. Weak, broad second-order peaks appeared near 3000 cm^{-1}.

4. CVD diamond film

The Raman spectrum for the CVD diamond film showed the first-order diamond peak at 1334 cm^{-1} and an additional broad asymmetric peak centered at 1568 cm^{-1} as shown in Fig. 4. Bandfitting revealed that this broad peak was composed of overlapping bands at 1357 and 1533 cm^{-1} (see Table II). The asymmetric peak indicated the presence of disordered regions, possibly composed of nondiamond carbon, in the CVD film.

5. Polyacetal

Polyacetal $(-CH_2-O-)_n$ was structurally unstable under 1000-keV Ar^+ bombardment because of its weak oxygen bonds. Residual gas analysis revealed that high concentrations of H_2 and H_2O molecules, in addition to monomers, dimers, and small amounts of multimers of acetal units, were emitted during bombardment. The implanted area was in the form of dull powdery soot and was very soft, indicating that long-range chemical bonding was destroyed. The implanted layer could be easily removed with a soft tissue. The Raman spectrum from the implanted region, shown in Fig. 5, resembled that of amor-

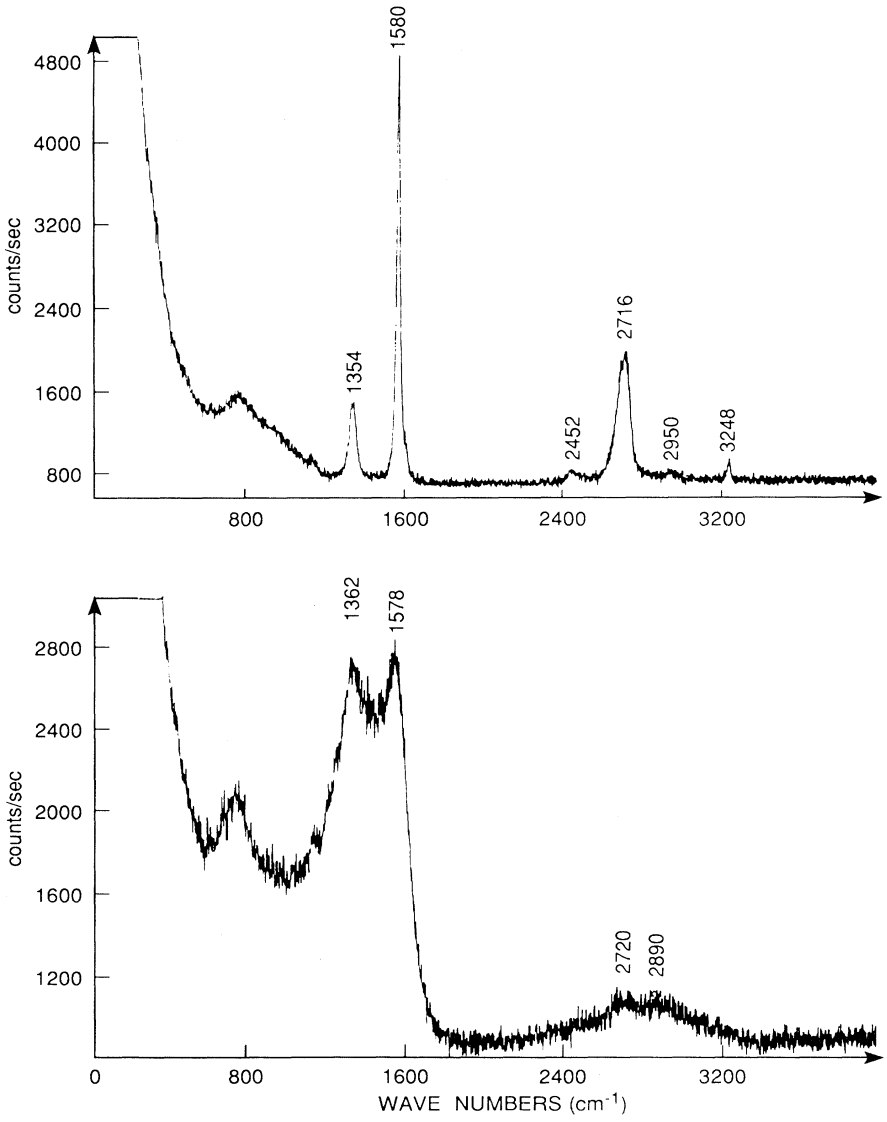

FIG. 1. Raman spectra of polycrystalline graphite (a) before and (b) after 200-keV Si^+-ion implantation.

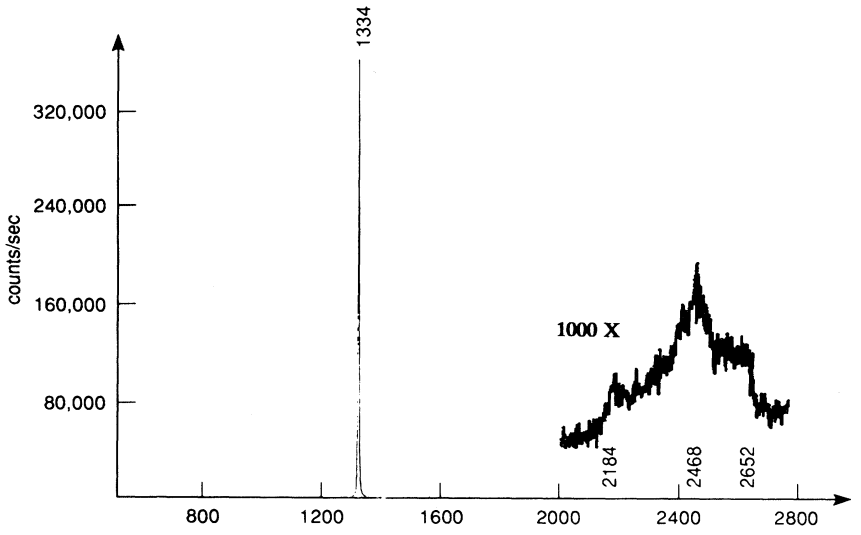

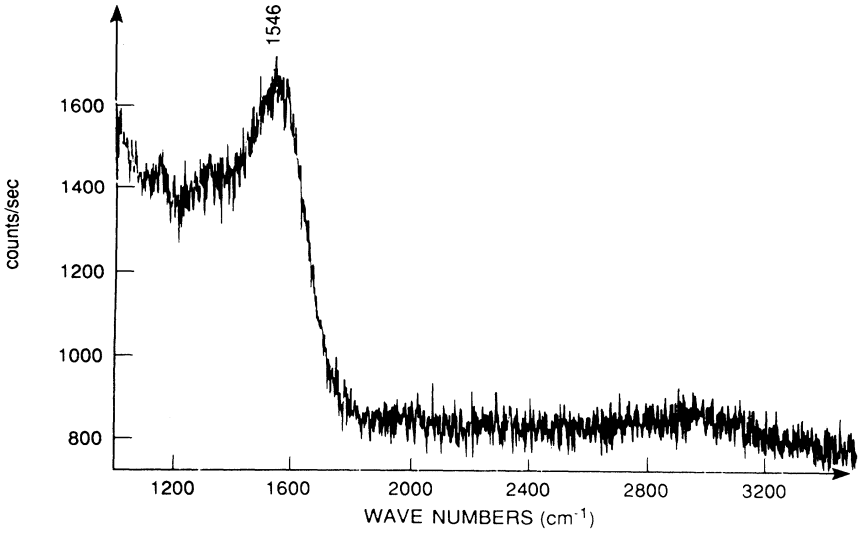

FIG. 2. Raman spectra of diamond (a) before and (b) after 1-MeV Ar^+-ion implantation.

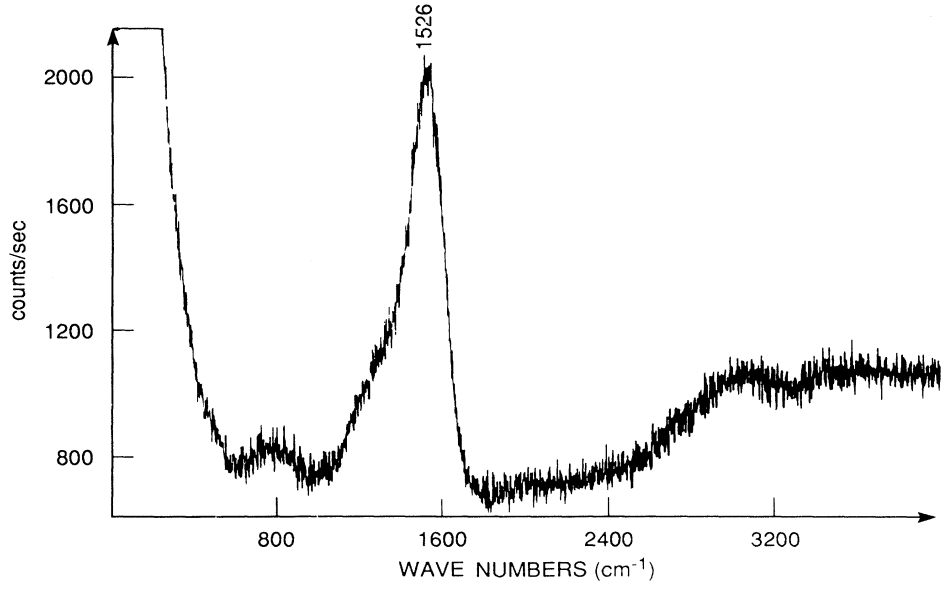

FIG. 3. Raman spectrum of DLC film.

TABLE II. Summary of bandfitting analysis for asymmetric peaks.

Materials	Peak position (cm^{-1})	Peak height ratio (H_D/H_G)	Peak area ratio (I_D/I_G)
Diamond 1000-keV Ar^+	1417(*D*) 1569(*G*)	0.61	1.05
DLC	1357(*D*) 1533(*G*)	0.44	0.90
CVD diamond	1355(*D*) 1542(*G*)	0.54	0.59
PS 1000-keV Ar^+ 8×10^{18} m^{-2}	1407(*D*) 1573(*G*)	0.72	1.78
PS 1000-keV Ar^+ 2.7×10^{19} m^{-2}	1414(*D*) 1561(*G*)	0.97	2.02
PS 1000-keV Ar^+ 5.4×10^{19} m^{-2}	1414(*D*) 1559(*G*)	0.92	1.63

phous carbon with the *D* line at 1368 cm^{-1} and the *G* line at 1604 cm^{-1}. The spectrum in Fig. 5 is after background subtraction to remove the strong luminescence that partially obscured the Raman bands. It should be noted that the *G* line is higher in frequency than that of polycrystalline graphite (1580 cm^{-1}). This is another consequence of relaxation of the wave-vector conservation selection rule as a result of defects or microcrystallinity. In this case, contributions to Raman scattering from normally forbidden phonons at or near the zone edge at approximately 1620 cm^{-1} cause an apparent upward shift in the frequency of *G* line.[20]

6. *Polystyrene*

Residual gas analysis revealed that the major species emitted during Ar^+ bombardment of polystyrene $(\text{-}CH_2\text{-}CH\phi\text{-})_n$ were H_2, CH_4, C_2H_2, C_2H_5, and C_6H_6. Because of the predominant loss of hydrogen, the residual material became a carbon-rich glassy phase. The modified surface changed from colorless to brown and eventually became completely dark at high fluences. The surface of the modified polystyrene (PS) became harder with increasing ion fluence and energy, and had a metallic luster which was not observed for polyacetal.

The first-order Raman spectrum of the 200-keV Ar^+ implanted specimen resembled that of polyacetal at the lowest fluence. Figure 6 shows the *D* line appearing near 1384 cm^{-1} and the *G* line near 1604 cm^{-1} for a fluence of 8×10^{18} ions/m^2. When the fluence was increased to 5.4×10^{19} ions/m^2, the spectrum became more like that of amorphous carbon. The *D* and *G* lines merged together forming an asymmetric peak with the maximum peak position at $\sim$1540 cm^{-1}.

For 1000-keV Ar^+ implantation at the lowest fluence (8×10^{18} ions/m^2), two Raman peaks were again observed, with the *D* line at 1374 cm^{-1} and the *G* line at 1566 cm^{-1} as shown in Fig. 7. Interestingly, the *G* line is at a much lower wave number than for the 200-keV implantation at the same fluence (1604 cm^{-1}), and even lower than the frequency for unimplanted graphite (1580 cm^{-1}). With increasing fluence, the *G* line shifted continuously to lower wave number while the *D* line shifted higher until the two peaks merged into a broad, asymmetric band as shown in Fig. 7. Bandfitting results for the asymmetric peaks are given in Table II. In general, the Raman spectra from Ar^+-implanted polystyrene resembled the spectrum of polycrystalline graphite for the low-energy and low-fluence implantations, but were similar to the spectrum of amorphous carbon with increasing ion energy and fluence.

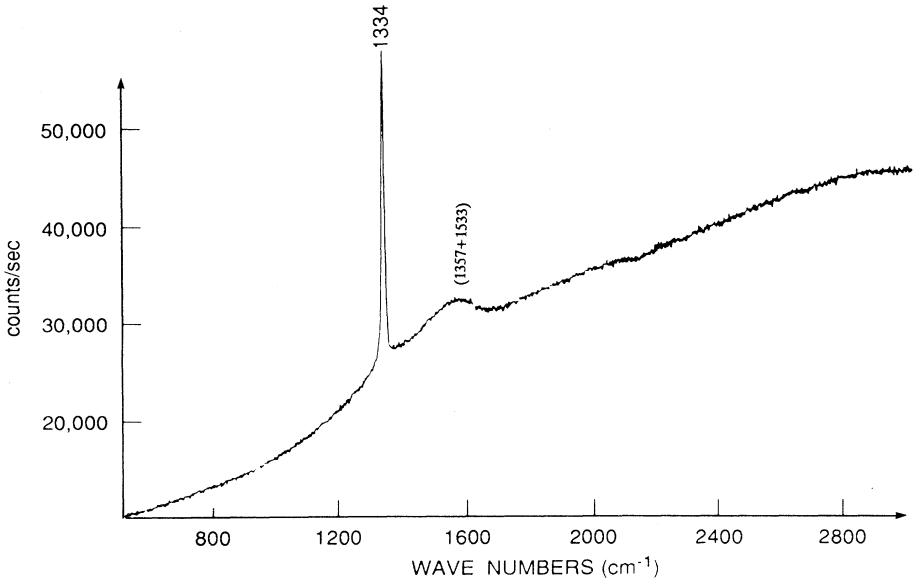

FIG. 4. Raman spectrum of FACVD film. The analysis indicates that the broad asymmetric peak is a superposition of 1357 and 1533 bands.

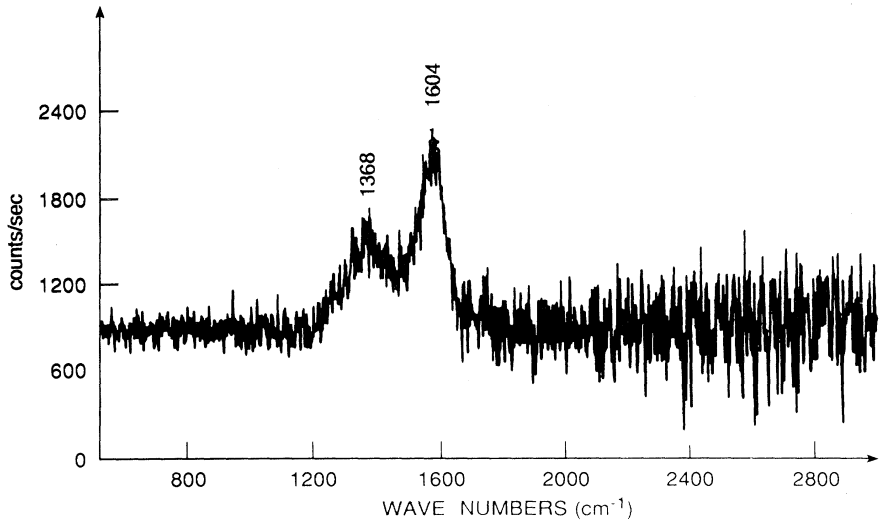

FIG. 5. Raman spectrum of polyacetal after 1-MeV Ar^+-ion implantation.

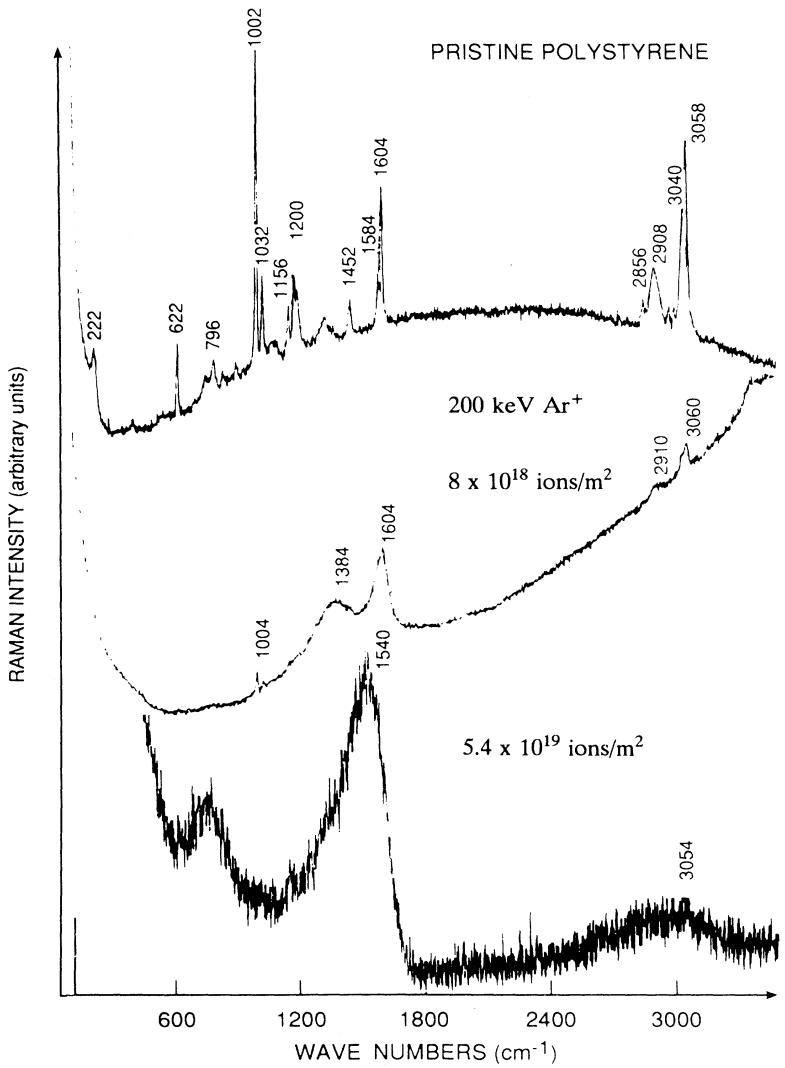

FIG. 6. Raman spectra of polystyrene before and after 200-keV Ar^+-ion implantation.

B. Hardness

One of the most striking differences between different forms of carbon is hardness. Hardness data from this study and from other sources are summarized in Table III. Hardness values of pristine and Ar-implanted diamond were measured using the Knoop indentation technique with a 1-N normal load and a 15-s dwell time. Calculations from the measured diagonals yielded hardness values of 222 GPa for pristine and 39 GPa for the implanted diamond, indicating that Ar implantation had softened the diamond by a factor of 5.7. The hardness of implanted diamond may have been slightly overestimated due to the undamaged diamond beneath the surface film. The penetration depth of the Knoop indenter was ~ 0.63 μm, which is approximately the ion penetration depth. Hardness values in the range 55–131 GPa have been reported for diamond depending on the quality and orientation.[29,30] It should be noted that the hardness of Ar-implanted diamond is still extremely high compared to

TABLE III. Summary of hardness data.

Materials	Ion energy and fluence (keV, ions/m^2)	Hardness (GPa)
Diamond		
Pristine		222
Implanted	1000, 2×10^{20} (Ar)	39
Graphite		
Pristine		0.08
Implanted	200, 1.6×10^{19} (Si)	0.12
DLC Film		0.62
Polystyrene		
Pristine		0.32
Implanted	200, 8×10^{18} (Ar)	1.3
	200, 2.7×10^{19} (Ar)	1.7
	200, 5.4×10^{19} (Ar)	1.8
	1000, 8×10^{18} (Ar)	7.5
	1000, 2.7×10^{19} (Ar)	9.5
	1000, 5.4×10^{19} (Ar)	12.5

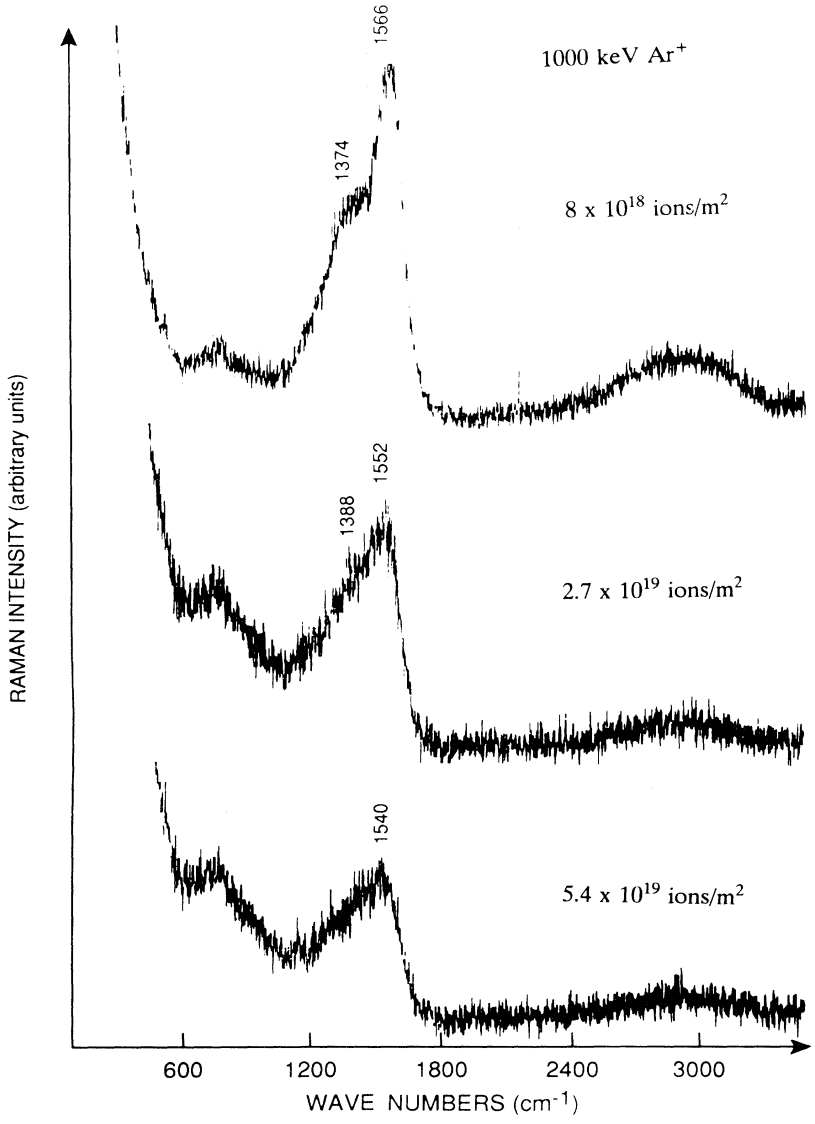

FIG. 7. Raman spectra of polystyrene as a function of 1-MeV Ar^+-ion fluence.

that of other materials. This is probably because most chemical bonds were still intact although they may have been severely distorted.

The hardness of graphite, the DLC film, and implanted PS was measured using a nanoindentation method[31] which is used to probe subsurface hardness. Five indents were made for each material, and the results were remarkably reproducible (to within a few percent difference). The hardness of pristine and Si-implanted graphite were very similar, having values of 0.08 and 0.12 GPa, respectively. The hardness of the DLC film was about 0.62 GPa, substantially higher than that of graphite and vapor-deposited *a*-C films. In the case of evaporated *a*-C films, hardness values were in the range 0.2–0.5 GPa.[32–34]

The hardness of Ar-implanted PS increased with ion fluence and energy, having values of 0.32 GPa for pristine, 1.3 GPa at 8×10^{18} ions/m^2, 1.7 GPa at 2.7×10^{19} ions/m^2, and 1.8 GPa at 5.4×10^{19} ions/m^2 for 200-keV Ar^+ irradiation. In the case of 1000-keV Ar^+ implantation of PS, hardness values were 7.5, 9.5, and 12.5 GPa for the same corresponding fluences. At the higher energy, hardness values of Ar^+-implanted PS approached those of CVD diamond films. In this study, the hardness of the CVD diamond film was not measured because of surface roughness but reported values range from 12 to 60 GPa.[32,34–36]

IV. DISCUSSION

Raman spectra from a wide variety of carbons produced by various techniques have been examined in this study. Relevant studies from the large body of work dealing with carbon are reviewed and compared with the present data in Tables IV and V. Table IV summarizes *D*- and *G*-line positions of the Raman spectra of diamond, single-crystal graphite, polycrystalline graphite, hydrogenated and unhydrogenated amorphous carbon,

TABLE IV. Raman spectra for various carbon compounds [*A*, asymmetric peak; *B*, broad peak (*D* and *G* lines are generally overlapped in the middle making a twin peak); *S*, sharp peak].

Materials	*D* line (cm^{-1})	*G* line (cm^{-1})	Reference
Natural diamond	$(1332)_S$[a]		25,11
	$(1336)_S$[a]		14
	$(1334)_S$[a]		This work
Graphite			
Single crystal		$(1580)_S$	11,41
		$(1585)_S$	21
		$(1584)_S$	14
		$(1575)_S$	19
Small crystallite	$(1360)_B$	$(1620)_B$	23
Charcoal	$(1360)_B$	$(1584)_B$	11
Polycrystalline	$(1355)_B$	$(1575)_B$	19
Graphite	$(1360)_B$	$(1580)_B$	41
	$(1354)_B$	$(1580)_B$	This work
a-C, graphite			
e-Beam evap. or	$(1360)_B$	$(1580)_B$	41
Ar sputtered		$(1550)_A$	37
900 C annealed	$(1350)_B$	$(1580)_B$	9
	$(1353)_B$	$(1598)_B$	38
a-C:H, graphite			
Ar sputtered in H_2		$(1580)_A$	37
500 °C annealed	$(1370)_B$	$(1590)_B$	
a-C:H, DLC			
rf discharge in		$(1520)_A$	10
CH_4		$(1357+1533)_A$	This work
CVD diamond			
FACVD, CH_4/H_2	$(1332)_S$[a]		13, 15, and this work
	$(1333)_S$[a]		
	$(1334)_S$[a]	$(1355+1542)_A$	
MPCVD, CH_4/H_2	$(133)_S$[a]	$(1550)_A$	17
Flame, C_2H_2/O_2	$(1334)^a_S+(1342)_B$	$(1576)_B$	16

[a]In general, *D* line designates a disorder peak, not the diamond peak.

DLC films prepared by rf discharge, and diamond films prepared by CVD methods. Table V summarizes the same type of Raman information for ion-implanted carbon compounds. Appropriate references are listed in the tables.

From this work and the studies reviewed in Tables IV and V, it was concluded that carbon phases can be placed into one of three general categories, depending on the bonding state. First, diamond and single-crystal graphite have single, sharp first-order bands at 1332 and 1580 cm^{-1}, respectively, which are highly characteristic features of the two allotropes of carbon with very long-range order. Second, graphitic carbon exhibiting finite crystal size effects is a distinct carbon form that is produced by many methods. Annealing of amorphous carbon at high temperature,[9,23,37,38] ion implantation of polymers such as polyacetal and PS (at low fluence and energy), and ion implantation of single-crystal graphite[22,39,40] are all examples of methods of producing graphite exhibiting finite crystal size effects. Raman scattering from these types of carbons showed the disorder induced *D* line near 1360 cm^{-1} along with the *G* line near 1580 cm^{-1}. When the crystallite size became smaller, both Raman lines became broader and the *G* line became asymmetric with a shift to higher wave number. The third general category is amorphous carbon in which the *D* and *G* lines coalesce into a weak, broad asymmetric peak with a maximum in the 1500–1560 cm^{-1} region. The shift of the *D* line to higher frequency along with the *G* line moving to lower frequency is distinctly different from the finite crystal size effects discussed above. Two types of amorphous carbon were identified in this study; soft carbon such as Si-implanted graphite and *e*-beam and sputter-deposited carbon,[9,37,41] and hard carbons such as DLC, Ar-implanted diamond, and some ion-implanted polymers.

TABLE V. Raman spectra of ion-implanted carbon compounds [*A*, asymmetric peak; *B*, broad peak (*D* and *G* lines are generally overlapped, making a twin band)].

Materials	*D* line (cm^{-1})	*G* line (cm^{-1})	Reference
Diamond, 1000-keV Ar^+			
2×10^{20} m^{-2}		$(1417+1569)_A$	This work
Ion implanted	(1332)	$(1400-1600)_A$	42
Graphite			
100 keV B, $10^{18}-10^{19}$ m^{-2}	$(1360)_B$	$(1580)_B$[a]	22
40–200 keV He, 10^{19} m^{-2}	$(1360)_B$	$(1580)_B$[a]	22
200-keV Si, 1.6×10^{19} m^{-2}	$(1362)_B$	$(1578)_B$	This work
Ion implanted		$(1400-1600)_A$	42
PE, 60-keV O_2^+			45
2.5×10^{19} m^{-2}	$(1300-1400)_B$	$(1550-1600)_B$	
1×10^{20} m^{-2}	$(1300-1400)_B$	$(1550-1600_B$	
Tefzel, 420, 700, 640 keV			4
(B,N,C), 1.2×10^{20} m^{-2}	$(1356)_B$	$(1588)_B$	
Kapton, 150-keV Ar			46
1×10^{19} m^{-2}	$(1400)_B$	$(1600)_B$	
1×10^{29} m^{-2}	$(1400)_B$	$(1580)_B$	
PS, 240-KeV Ar			39
5×10^{19} m^{-2}		$(1500-1600)_A$	
4×10^{20} m^{-2}		$(1500-1600)_A$	
PS, 200-keV Ar			This work
8×10^{18} m^{-2}	$(1384)_B$	$(1604)_B$	
5.4×10^{19} m^{-2}		$(1540)_A$	
PS, 1000-keV Ar			This work
8×10^{18} m^{-2}	$(1374)_B$	$(1566)_B$	
2.7×10^{19} m^{-2}	$(1388)_B$	$(1552)_B$	
5.4×10^{19} m^{-2}		$(1414+1559)_A$	
Polyacetal, 1000-keV Ar			This work
1.6×10^{20} m^{-2}	$(1368)_B$	$(1604)_B$	

[a]Additional small peak was observed at 1620 cm^{-1}. For B implantation, the *G* line shifted to higher wave numbers with decreasing crystallite sizes when ion dose increased. For He implantation, the *G* line shifted to lower wave numbers with increasing crystallite sizes when ion energy was increased.

The Raman scattering data indicates that carbon phases can be uniquely classified into the three distinct types outlined above, depending upon the shape and frequency of the *D* and *G* lines. As such, a new classification scheme based on the Raman peak positions is proposed. Materials are categorized as being graphitic when the *G* line is equal to or greater than 1575 cm^{-1}, the frequency observed for single crystal, natural graphite.[19] In this case, the *D* line remains at approximately 1360 cm^{-1}. Average particles sizes are larger than 1 nm, based on the data reviewed in Table IV. Carbon is categorized as being amorphous when the *G* line is below 1575 cm^{-1} and the *D* line moves higher in frequency (typically to 1400 cm^{-1} or higher). In general, when particle sizes are less than 1 nm, x-ray or electron-diffraction methods fail to identify the crystalline features. Raman scattering is a more useful criterion for determining the degree of disorder in carbon in such cases.

Although there were subtle differences in peak positions and peak shapes depending upon the material and experimental parameters, *a*-C, *a*-C:H, DLC, Si-implanted graphite, Ar-implanted diamond, and ion-implanted polymers, all showed similar Raman spectra, suggesting that they all have common structural features despite the difference in chemical bonding of the pristine materials. As a result, Raman scattering could not be used to distinguish between amorphous carbons produced by different techniques. Interestingly, however, the disordered diamond was much harder than disordered graphite (39 GPa vs 0.12 GPa) hinting that the three-dimensional network of chemical bonds was still intact in diamond. The presence of other elements (e.g., oxygen and nitrogen in Kapton®, fluorine in Tefzel®, and hydrogen in DLC, PE, and PS) had no noticeable effect on the Raman spectrum of amorphous carbon. Amorphous carbons apparently have a large capacity to accommodate various defects and impurities due to their more random structure and, as such, the Raman spectrum, dominated by scattering from a carbon arrangement common to all of these materials, is very similar.

There have been numerous attempts by researchers to establish the level of sp^3 bonding in various amorphous carbons.[1,11,24,37,38] This is particularly true for the hard carbon films in which a significant level of sp^3 bonding would help explain the hardness.[9–17] From the Raman spectra, it is clear that good quality CVD diamond films have a definite diamond structure with almost no sp^2 bonding. However, the level of sp^2 and sp^3 bonding in various amorphous carbons is still the subject of debate. A large fraction of sp^3 bonds would be expected to remain in the implanted diamond as shown by ion channeling data and by retention of its extreme hardness (see Table III), while implanted graphite would be expected to be composed of a large fraction of sp^2 bonds. Yet both materials had similar Raman spectra (graphitelike spectrum),[42] which, in turn, were similar to the spectra of DLC and the heavily implanted polymers. Interestingly, the Raman spectrum of each of these materials exhibits a broad, asymmetric peak in the 1500–1575 cm^{-1} region, which does not correspond to a maximum in the phonon density of states of either graphite (sp^2) or diamond (sp^3).[9,20]

Several models for the structure of amorphous carbon have been proposed.[2,11,24] The emerging picture from this and other work is that many amorphous carbons consist of an intricate network of single, double, and triple bonds and their conjugate forms which are interconnected in a random fashion. Graphitic sp^2 planar regions are often interconnected via tetragonally bonded sp^3 bonds allowing gradual changes in planar orientations. Bond angles are greatly distorted in such structures. In hydrogenated carbon, about 15 different types of bonds have been identified by infrared absorption including $-CH_3$, $=CH_2$, and $\equiv CH$ bonds together with other *sp*, sp^2, and sp^3 hybridizations and conjugated bonds.[2] Figure 8 shows infrared spectra of polystyrene before and after implantation with 1-MeV Ar^+ to a fluence of 5.4×10^{19} ions/m^2.[43] The distinct vibrational modes of pristine PS were replaced by a broad feature between approximately 800 and 1800 cm^{-1} after implantation. A wide range of C-C stretching and CH bending modes,

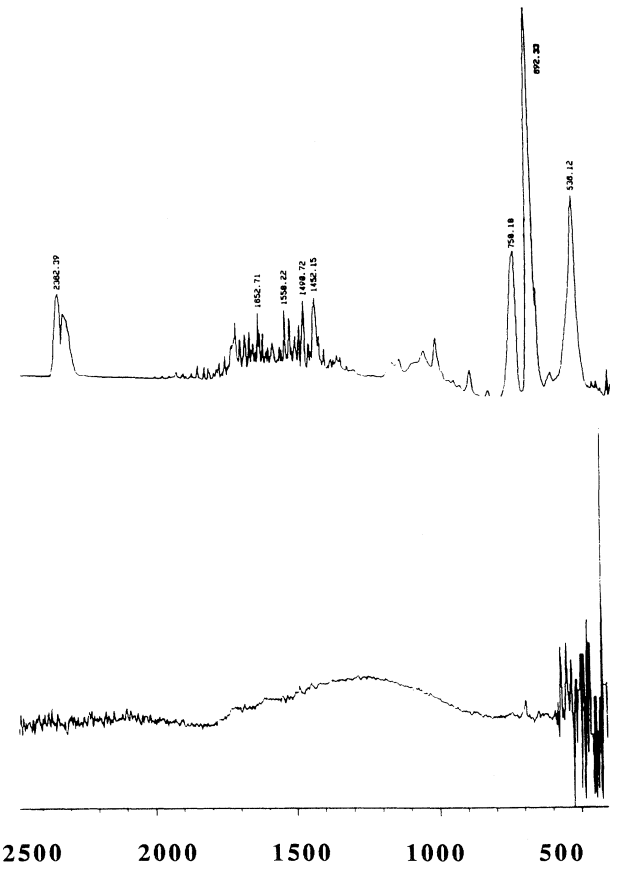

FIG. 8. Infrared spectra of pristine (above) and Ar^+-ion-implanted polystyrene to a fluence of 5.4×10^{19} ions/m^2 at 1000 keV (Ref. 43) (below). For the implanted specimen, the unaffected regions were eliminated by dissolving in a solvent and the spectrum was obtained from the bombarded region only.

probably with a great deal of bond angle distortion, are the dominant species observed in the spectrum of implanted PS. Recently, the presence of C_{60} fullerene molecules was also observed in ion-implanted polymeric materials.[44]

In general, most experimental results suggest that there is no particular bonding type that necessarily dominates in many amorphous carbons, especially for ion-implanted materials. While more hydrogenated carbon atoms are expected in DLC and ion-beam-treated polymers, more sp^3 bonds are expected in damaged diamond and more sp^2 bonds in graphite as discussed above. Because all of these show a similar response to Raman scattering, it seems plausible that sp^3 or sp^2 bonds in these amorphous structures have severely distorted bond angles (and bond lengths). In such cases, the Raman scattering intensity decreases and the peaks broaden because of the loss of translational symmetry.

A downward shift of the G line with increasing sp^3 bonds was predicted in Beeman *et al.*'s theoretical work,[24] which was based on lattice dynamic calculations using the valence force field model. In their random-network model, peak broadening and shifting was related to the degree of disorder and the relative proportion of sp^2 and sp^3 bonds. Current experimental results, however, indicate that the shift to lower frequency occurs when carbon becomes disordered, regardless of the initial state (e.g., diamond, graphite, or polymers). For example, the highly characteristic diamond peak at 1332 cm^{-1} was severely attenuated by ion implantation and replaced by a broad asymmetric peak which was very similar to the peak observed for other amorphous carbons. It is certainly possible that a significant level of sp^3 bonding exists in highly disordered carbons, but such a conclusion is not supported by the Raman results in this work.

Despite the similar response to Raman scattering, amorphous carbons exhibited quite different physical properties, particularly hardness, depending upon preparation conditions. Since hardness is a manifestation of the degree of chemical bonding in three dimensions, differences in hardness in these materials are thought to arise from variations in the degree of crosslinking. As an example, *e*-beam evaporated or sputter-deposited films are produced by condensation of carbon atoms from the vapor phase. The sizes of the clusters which nucleate generally vary with substrate temperature. At low temperatures, small clusters of randomly bonded carbon atoms aggregate without establishing long-range chemical bonds, and result in carbon films with very low hardness. On the other hand, much harder DLC films are grown from ionized carbon deposition which led to better long-range chemical bonding. The results of this study indicate that although there are distinct differences in physical properties and long-range bonding among the various amorphous carbons, Raman scattering is not sensitive to these differences. Properties related to the degree of three-dimensional connectivity are better determined by other methods such as hardness measurements.

V. CONCLUSIONS

Raman scattering studies were conducted on diamond, graphite, and several polymers to investigate the nature of chemical bonds in various carbon-based materials. CVD diamond and DLC films were also examined in the as-prepared condition for comparison with the ion-bombarded materials. It was shown that a shift of the G line to frequencies above 1575 cm^{-1} is indicative of crystalline graphite, whereas a shift below 1575 cm^{-1} can be attributed to amorphization (or the onset of amorphization). Although all disordered carbons had similar Raman spectra, the D and G lines tended to be well-separated, distinct peaks for the more graphite materials and to merge into a broad asymmetric peak for the highly disordered carbons.

Raman spectra of ion-implanted diamond, polycrystalline graphite, polymers, DLC, *e*-beam evaporated graphite, and sputter-deposited graphite are similar. Each of these materials has a carbon framework that is in a highly disordered, distorted state, and no evidence for significant levels of pure sp^2 or sp^3 bonded carbon could be found. Experimental evidence suggests that there is no clear correlation between hardness and sp^3 bonding in amorphous carbons, but rather, hardness is related to the level of three-dimensional connectivity involving many types of distorted bonds.

ACKNOWLEDGMENTS

Research was sponsored in part, by the U.S. Department of Energy, Assistant Secretary of Conservation and Renewable Energy, Office of Industrial Technologies, Advanced Industrial Concepts (AIC) Materials Program, and in part by the Division of Materials Science, U.S. Department of Energy under Contrast No. DE-AC05-84OR21400 with Martin Marietta Energy Systems, Inc. We would like to thank Dr. R. E. Clausing for lending DLC and CVD films for evaluations. We also would like to thank Dr. D. F. Pedraza, Dr. George Begun, and Dr. Norman R. Smyrl for technical review of the manuscript. One of the authors (G.R.R.) was supported by the Oak Ridge Institute for Science and Education.

[1]Hsiao-chu Tsai and D. B. Bogy, J. Vac. Sci. Technol. A **5**, 3287 (1987).

[2]J. Robertson, Adv. Phys. **35**, 317 (1986).

[3]Diamond and Diamond-like Films and Coatings, Vol. 266 of *NATO Advanced Study Institute Series: Physics,* edited by Robert E. Clausing, Linda L. Horton, John C. Angus, and Peter Koidl (Plenum, New York, 1991).

[4]E. H. Lee, M. B. Lewis, P. J. Blau, and L. K. Mansur, J. Mater. Res. **6**, 610 (1991).

[5]Y. Lee, E. H. Lee, and L. K. Mansur, Surf. Coatings Tech. **51**, 267 (1992).

[6]E. H. Lee, G. R. Rao, and L. K. Mansur, J. Mater. Res. **7**, 1900 (1992).

[7]T. Venkatesan, Nucl. Instrum. Methods Phys. Res. B **7/8**, 461

(1985).
[8]J. D. Carlson, J. E. Bares, A. M. Guzman, and P. P. Pronko, Nucl. Instrum. Methods Phys. Res. B **7/8**, 507 (1985).
[9]N. Wada, P. J. Gaczi, and S. A. Solin, J. Non-Crystalline Solids **35&36**, 543 (1980).
[10]M. Ramsteiner, J. Wagner, C. Wild, and P. Koidl, J. Appl. Phys. **62**, 729 (1987).
[11]Diane S. Knight and William B. White, J. Mater. Res. **4**, 385 (1989).
[12]J. Davenas, P. Thevenard, G. Boiteux, M. Fallavier, and X. L. Lu, Nucl. Instrum. Methods Phys. Res. B **46**, 322 (1990).
[13]H. A. Hoff, A. A. Morrish, J. E. Butler, and B. B. Rath, J. Mater. Res. **5**, 2572 (1990).
[14]L. S. Plano and F. Adar, Proc. SPIE Int. Soc. Opt. Eng. **120**, 376 (1990).
[15]David G. K. Jeng, H. S. Tuan, James E. Butler, Robert F. Salat, and Glenn J. Fricano, in *Diamond and Diamond-like Films and Coatings* (Ref. 3), p. 627.
[16]P. S. Nielson, K. Madsen, P. Balslev, and P. L. Hansen, in *Diamond and Diamond-like Films and Coatings* (Ref. 3), p. 745.
[17]Nubuo Setaka, in *Diamond and Diamond-like Films and Coatings* (Ref. 3), p. 875.
[18]M. B. Lewis, W. R. Allen, R. A. Buhl, N. H. Packan, S. W. Cook, and L. K. Mansur, Nucl. Instrum. Methods Phys. Res. B **43**, 243 (1989).
[19]F. Tuinstra and J. L. Koenig, J. Chem. Phys. **53**, 1126 (1970).
[20]R. J. Nemanich and S. A. Solin, Phys. Rev. B **20**, 392 (1979).
[21]R. J. Nemanich and G. Lucovsky, Solid State Commun. **23**, 117 (1977).
[22]B. S. Elman, M. S. Dresselhaus, G. Dresselhaus, E. W. Maby, and H. Mazurek, Phys. Rev. B **24**, 1017 (1981).
[23]P. Lespade, R. Al-Jishi, and M. S. Dresselhaus, Carbon **20**, 427 (1982).
[24]D. Beeman, J. Silverman, R. Lynds, and M. R. Anderson, Phys. Rev. B **30**, 870 (1984).
[25]M. H. Grimsditch and A. K. Ramdas, Phys. Rev. B **11**, 3139 (1975).
[26]S. A. Solin and A. K. Ramdas, Phys. Rev. B **1**, 1687 (1970).
[27]W. H. Allen and E. H. Lee, in *Beam-Solid Interactions: Fundamentals and Applications,* edited by Michael Natasi, Lloyd R. Harriott, Nicole Herbots, and Robert S. Averback, MRS Symposium Proceedings No. 279 (Materials Research Society, Pittsburgh, 1993), p. 333.
[28]J. D. Hunn, M. L. Swanson, E. A. Hill, N. R. Parikh, and G. Hudson, in *New Diamond Science and Technology,* edited by Russell Messier, Jeffrey T. Glass, James E. Butler, and Rustum Roy, MRS Symposia Proceedings of the Second International Conference (Materials Research Society, Pittsburgh, 1991), p. 929.
[29]R. M. Chrenko and H. M. Strong (unpublished).
[30]C. A. Brooks, *The Properties of Diamond,* edited by J. E. Field (Academic, London, 1979), p. 383.
[31]E. H. Lee, Y. Lee, W. C. Oliver, and L. K. Mansur, J. Mater. Res. **8**, 377 (1993).
[32]B. Disher and G. Brandt, Industrial Diamond Rev. **3**, 131 (1985).
[33]J. Hauser, Solid State Commun. **17**, 1577 (1975).
[34]J. Fink, T. Muller-Heinzerling, J. Pfluger, A. Bubenzer, P. Koidl, and G. Crecelius, Solid State Commun. **47**, 887 (1983).
[35]S. Kaplan, F. Jansen, and M. Machonkin, Appl. Phys. Lett. **47**, 750 (1985).
[36]C. Weissmantel, K. Bewilogua, K. Breuer, D. Dietrich, U. Ebersbach, H. J. Erler, B. Rau, and G. Riessen, Thin Solid Films **96**, 31 (1982).
[37]S. K. Hark, M. A. Machonkin, F. Jansen, M. A. Slade, and B. A. Weinstein, in *Optical Effects in Amorphous Semiconductors (Snowbird, UT),* Proceedings of the International Topical Conference on Optical Effects in Amorphous Semiconductors, edited by P. C. Taylor and S. G. Bishop, AIP Conf. Proc. No. **120** (AIP, New York, 1984), p. 465.
[38]R. O. Dillon, J. A. Woollam, and V. Katkanant, Phys. Rev. B **29**, 3482 (1984).
[39]L. Calcagno and G. Foti, Nucl. Instrum. Methods Phys. Res. B **59/60**, 1153 (1991).
[40]B. S. Elman, M. Shayegan, M. S. Dresselhaus, H. Mazurek, and G. Dresselhaus, Phys. Rev. B **25**, 4142 (1982).
[41]M. Nakamizo, R. Kammereck, and P. L. Walker, Jr., Carbon **12**, 259 (1974).
[42]J. E. Smith, Jr., M. H. Brodsky, B. L. Crowder, and M. I. Nathan, J. Non-Cryst. Solids, **8-10**, 179 (1972).
[43]G. R. Rao and E. H. Lee (unpublished).
[44]R. E. Johnson and Bo U. R. Sundquist, Phys. Today **45**, 28 (1992).
[45]A. Ishitani, K. Shoda, H. Ishida, T. Watanabe, and K. Yoshida, Nucl. Instrum. Methods Phys. Res. B **39**, 783 (1989).
[46]K. Yoshida and M. Iwaki, Nucl. Instrum. Methods Phys. Res. B **19/20**, 878 (1987).